Physics Letters B 318 (1993) 424–432
North-Holland

PHYSICS LETTERS B

Solid on solid on fluid lattices

C.F. Baillie

Physics Dept., University of Colorado, Boulder, CO 80309, USA

W. Janke

Institut für Physik, Johannes Gutenberg Universität , D-55099 Mainz, Germany

and

D.A. Johnston

PTHE, Université Paris Sud, Bâtiment 211, F-91405 Orsay, France[1]
and Dept. of Mathematics, Heriot-Watt University, Edinburgh, EH14 4AS, Scotland, UK[2]

Received 31 August 1993; revised manuscript received 13 October 1993
Editor: P.V. Landshoff

We perform simulations of a discrete gaussian solid on solid (DGSOS) model on dynamical ϕ^3 graphs, which is equivalent to coupling the model to 2d quantum gravity, using the cluster algorithms recently developed by Evertz et al. for use on fixed lattices. We find evidence from the growth of the width-squared in the rough phase of KT-like behaviour, which is consistent with theoretical expectations. We also investigate the cluster statistics, dynamical critical exponent and lattice properties, and compare these with the dual XY model.

1. Introduction

Following the work in [1,2] in the continuum Liouville theory formalism and the vast recent output of results in the context of matrix models [3] it is now clear that one can calculate the critical exponents for various $c \leqslant 1$ conformal field theories coupled to 2d quantum gravity given the conformal weights of operators in the "bare" theories without gravity. The coupling to 2d quantum gravity can be incorporated in discrete simulations of such models by having the matter live on, and interact with, a dynamical lattice – typically a dynamical triangulation or the dual dynamical ϕ^3 graphs. The Ising model can be solved exactly on dynamical ϕ^3 and ϕ^4 graphs [4], giving exponents in agreement with the continuum approach, and these results are also backed up by numerical simulations, as are the exponent values for 3 and 4 state Potts models coupled to 2d gravity [5]. For $c > 1$ the matrix models can no longer be exactly solved and the continuum approach breaks down, but numerical simulations show no obvious pathologies and neither do extrapolations from exactly evaluated partition functions for small numbers of points [6,7].

In view of this the borderline case of $c = 1$, exemplified by the 4 state Potts model or the XY model, is of particular interest. On a fixed lattice the XY model, whose partition function is

$$Z = \prod_i \int \mathrm{d}\theta_i \exp\left(\beta \sum_{\langle ij \rangle} \cos(\theta_i - \theta_j)\right), \qquad (1)$$

where the θ_i's are angular variables, is known to undergo a Kosterlitz–Thouless (KT) transition driven by the unbinding of vortex pair configurations [8]. The correlation length diverges as

[1] Address Sept. 1993–1994.
[2] Permanent address.

$$\xi = A_\xi \exp\left(\frac{B_\xi}{(T - T_c)^\nu}\right), \tag{2}$$

and the spin susceptibility as

$$\chi = A_\chi \exp\left(\frac{B_\chi}{(T - T_c)^\nu}\right), \tag{3}$$

where the exponent ν is predicted to be 1/2. The KT theory also predicts the correlation function critical exponent $\eta = 1/4$, where η is given by

$$\chi = C\xi^{2-\eta}. \tag{4}$$

It has proved notoriously difficult to confirm this behaviour numerically [9] though there is now a general consensus that the data supports a KT transition rather than possible alternatives such as a second order transition. On a dynamical lattice the theoretical predictions are that a KT transition persists [10] and the two simulations carried out to date appear to support this assertion [11,12].

Another class of lattice models, namely the solid on solid (SOS) models, are expected to display a KT roughening transition. Different variants of these models exist one of which, the body-centred solid on solid (BCSOS) model, is equivalent to a six vertex model which is exactly soluble and is known to have a KT transition [13]. Numerical evidence suggests that on fixed lattices other variants such as the dual of the XY model, the discrete gaussian solid on solid (DGSOS) model we consider here and the absolute value solid on solid (ASOS) model are in the same universality class [14]. The partition function for the DGSOS model on a fixed lattice is given by

$$Z = \sum_h \exp\left(-\beta \sum_{\langle i,j\rangle} (h_i - h_j)^2\right), \tag{5}$$

where the h's are integer heights at each lattice point and the sum in the exponent is over the edges in the lattice. In the ASOS model this is modified to

$$\sum_h \exp\left(-\beta \sum_{\langle i,j\rangle} |h_i - h_j|\right), \tag{6}$$

in the dual of the XY model to

$$\sum_h \prod_{\langle i,j\rangle} I_{|h_i - h_j|}(\beta), \tag{7}$$

where $I_{|h_i-h_j|}$ is a modified Bessel function, and in the BCSOS model to

$$\sum_h \exp\left(-\beta \sum_{[i,j]} |h_i - h_j|\right), \tag{8}$$

where i, j are now diagonal neighbours and nearest neighbours are constrained by $|h_i - h_j| = 1$. The models have a rough phase at low β separated from a smooth phase at high β by the KT transition. The width-squared of the surface, which can be defined by

$$\sigma^2 = \left\langle \frac{1}{N} \sum_i (h_i - \bar{h})^2 \right\rangle, \tag{9}$$

where $\bar{h}$ is the mean value of the h_i, is predicted by KT theory to diverge logarithmically in the rough phase with the number of points N:

$$\sigma^2 = \frac{T_{\text{eff}}}{d\pi} \log(N) + B, \tag{10}$$

where d is the fractal dimension of the lattice (we have substituted $L = N^{1/d}$). At the critical point $\beta = \beta_c$ KT predicts $T_{\text{eff}} = 2/\pi$ and as β approaches β_c from below $T_{\text{eff}} - 2/\pi \simeq (\beta_c - \beta)^{1/2}$. On fixed lattices it appears that it is possible to unambiguously verify eq. (10) for sufficiently small β but that the behaviour of T_{eff} as $\beta \to \beta_c$ cannot be fitted without including corrections in the formula for the width-squared coming from using a "running temperature" in the KT flow equations [14].

2. The simulation method

In this paper we simulate the DGSOS model on dynamical ϕ^3 graphs of spherical topology with a fixed number N of points and no tadpole or self-energy insertions which would correspond to degenerate triangulations on the direct lattice. The partition function is now

$$Z = \sum_{G^{(N)}} \sum_h \exp\left(-\beta \sum_{\langle i,j\rangle} G_{ij}^{(N)} (h_i - h_j)^2\right), \tag{11}$$

where $G_{ij}^{(N)}$ is the connectivity matrix of the graph. Our aims are threefold:

- We wish to see if the KT predictions are still valid when the SOS model is coupled to 2d quantum gravity, as they appear to be in the XY model case;
- We wish to investigate the efficiency of the cluster algorithms used in simulating the SOS models on dynamical lattices;
- We wish to see how the lattice characteristics of the SOS model compare with the Potts and XY models simulated previously.

To this end we simulate graphs with $N = 100, 200, 300, 400, 500, 1000, 2000, 5000, 10000$ points for a range of β values from 0.05 to 5.0. For each data point we carried out 10000 metropolis equilibration sweeps, followed by 50000 measurements. Before each set of measurements we carry out a number of Wolff updates using the H and I algorithms of Evertz et al. tuned so that $N_{\text{updates}} = 1/$ Cluster Size, as well as N local "flip" moves in the lattice. Test runs and our experience with simulating the Potts and XY models on dynamical lattices provided assurance that this was sufficient to allow for the lattice and the spin model to interact. To ensure detailed balance it is necessary to check that the rings at either end of the link being flipped have no links in common. The starting graphs came from the Tutte algorithm used to generate pure two-dimensional gravity meshes.

The cluster algorithms used in the simulations are of the so-called "valley to mountain reflection" type [14]. One chooses a reflection plane at height M and notes that all of the h_i may be written as $h_i = \sigma_i|h_i - M| + M$ where the $\sigma_i = \pm 1$ are embedded Ising variables determining whether the height h_i is above $(+)$ or below $(-)$ M. A cluster is then built by choosing a seed point and adding further links $\langle ij \rangle$ with the probability

$$P_{\text{add}} = 1 - q \exp\left(-\beta|h_i - M||h_j - M|(\sigma_i\sigma_j + 1)\right), \tag{12}$$

where $q \leqslant 1$. It is then flipped by reversing the sign of the embedded Ising variables in the cluster. The fixed lattice simulations in [14] revealed that the choice of the reflection plane M was crucial for the effectiveness of the algorithm, because the width-squared of the surfaces was not that great (in the region of 1–2) for values of β around β_c even for large lattices. One has to be careful to ensure that M is not picked too far away from the surface. If we take $q = 1$ in eq. (13) taking the reflection plane to pass through the seed point will generate only clusters of size 1 ("monomers") so we must choose some other point close to the seed. One possibility is to take $M = h_{\text{seed}} \pm 1/2$, where the plus and minus are chosen with equal probability, which was called the H algorithm (H = half-integer) in [14]. It was found that this algorithm, while ergodic, still had a dynamical critical exponent $z \simeq 1$. It was pointed out in [14] that single step islands, configurations where a set of points on the surface were a step above or below the background, could be created and destroyed by the H algorithm but not reflected by it. Such reflections would cost nothing in terms of the Boltzmann weights and are thus likely to be important for the dynamics. They should therefore be included by some means if one is trying to mimic the physically relevant degrees of freedom with the clusters. A possibility for doing this is to take $M = h_j$ where j is another randomly chosen point other than the seed on the surface, which was called the I algorithm (I = integer). This is no longer ergodic on its own as only even changes in heights will result from the reflections, but combining the H and I algorithms gives an ergodic algorithm that effectively eliminates critical slowing down on fixed lattices. Another possibility is to take $M = h_{\text{seed}}$ with $q < 1$ when $h_i = h_{\text{seed}}$, giving a so-called Q algorithm which could also be combined with the H algorithm to eliminate critical slowing down. For the sake of simplicity we concentrate here on combining the H and I algorithms in our simulations.

In the simulations we measured the width-squared, as defined in eq. (9), the energy

$$E = \frac{\beta}{N}\left\langle \sum_{\langle ij \rangle} (h_i - h_j)^2 \right\rangle, \tag{13}$$

the specific heat

$$C = N(\langle E^2 \rangle - \langle E \rangle^2), \tag{14}$$

autocorrelation functions for the energy and width-squared and the correlator

$$C_{ij} = \left\langle \frac{1}{n(r)} \sum_{ij} (h_i - h_j)^2 \delta(d_{ij} - r) \right\rangle, \tag{15}$$

where d_{ij} is the geodesic distance on the lattice between points i and j and

$$n(r) = \sum_{ij} \delta(d_{ij} - r) \qquad (16)$$

is the number of points at geodesic distance r. The size, diameter and number of boundary points of the two types of clusters and various characteristics of the lattice itself were also measured. In what follows we describe the results of these measurements.

3. Measurements on the SOS model

The energy and specific heat are plotted in fig. 1 for the various β values and system sizes simulated. The curve for the specific heat looks gratifyingly KT-like - there is no sign of an increasing peak with system size as one would expect for a second order transition. It is also clear that the behaviour of the model as $\beta \to 0$ is correctly being reproduced. In this limit the diverging width of the surface relative to the lattice size means that one has in effect real valued heights at each point instead of integers. We should thus see the behaviour of a single free real scalar field as $\beta \to 0$ and it is known from a simple scaling argument that both the energy and specific heat for this should be 1/2. Both the specific heat and energy curves in fig. 1 show this behaviour up to $\beta \simeq 1.5$. The phase transition point is not at the maximum in the specific heat curve for

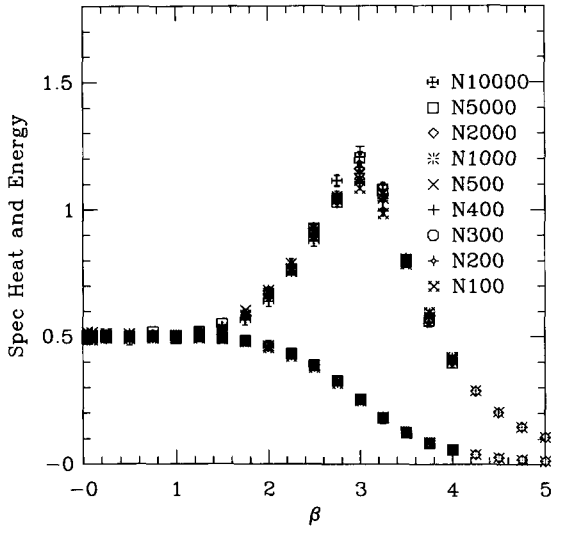

Fig. 1. The specific heat and energy for the various graph sizes plotted against β.

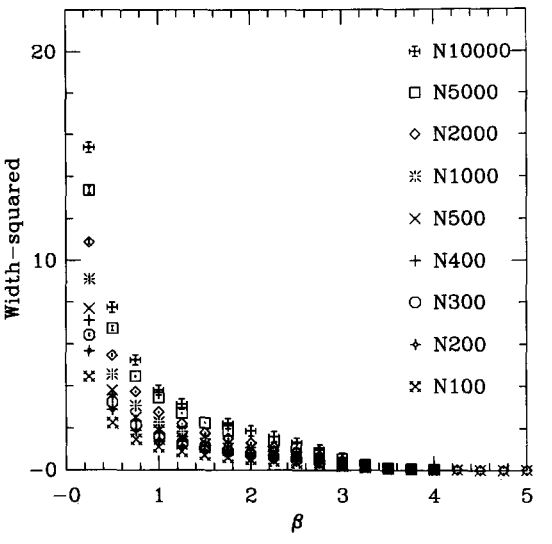

Fig. 2. The width-squared of the surfaces as defined in eq. (9). The lowest β values are not plotted in order to avoid compressing the scale.

a KT transition but using this as a rough guide, along with the onset of the divergence in the width-squared the critical region is in the region of, or just below, $\beta = 3$.

The scaling relation of eq. (10) for the width-squared, which is plotted in fig. 2 with the smallest β values dropped to avoid an overly large scale is also verified. In table 1 we show the results of fitting σ^2 to $A\log(N) + B$. As might be expected the fits are quite good deep in the rough phase but deteriorate as one approaches the transition point in the region of $\beta = 3$. We do not attempt to fit $A(= T_{\text{eff}}/d\pi)$ to $T_{\text{eff}} - 2/\pi \simeq (\beta_c - \beta)^{1/2}$ because of the aforementioned necessity of including corrections to this formula by introducing a "running temperature" in the KT flow equations. We do not have sufficient data near to the putative critical point from the current runs to fit accurately to this modified formula for the width-squared. As well as measuring the behaviour of the DGSOS model itself it is also interesting to investigate the algorithmic aspects of the simulation, in particular whether the mixed H and I cluster methods employed here are still efficient at reducing critical slowing down. In the case of fixed lattices it was found [14] that combining the H and I algorithms gave a very small, or perhaps even zero, value of the

Table 1
Fitted values of A and B.

β	A	B	χ^2
0.05	11.8(1)	−35(1)	7.3
0.10	6.57(8)	−22(1)	3.9
0.25	2.36(4)	−7.0(3)	2.6
0.50	1.16(2)	−3.4(1)	2.5
0.75	0.83(1)	−2.6(1)	4.1
1.00	0.61(1)	−1.9(1)	5.9
1.25	0.50(1)	−1.60(4)	4.4
1.50	0.36(1)	−0.95(2)	5.1
1.75	0.315(3)	−0.89(2)	4.3
2.00	0.270(3)	−0.76(2)	4.3
2.25	0.256(3)	−0.85(2)	6.5
2.50	0.207(3)	−0.67(2)	5.7
2.75	0.153(1)	−0.47(1)	7.3
3.00	0.091(1)	−0.23(1)	5.9

Table 2
Values of z/d for selected β.

β	z/d	χ^2
0.05	0.0018(1)	2.9
0.25	0.0007(1)	4.3
2.50	0.0018(1)	10
2.75	0.0089(3)	9
3.00	0.0027(1)	9

dynamical critical exponent z defined by $\tau \simeq L^z$, where L is the linear size of the system and τ is the autocorrelation time, for $\beta \leqslant \beta_c$[#1]. In our case we must use the definition $\tau \simeq N^{z/d}$ where d is again the fractal dimension of the lattice We find that z/d is very small for all of the β values we simulated, some typical values are listed in table 2. If we assume that the fractal dimension is $\simeq 2.6$, which is what we measure in a naive counting of the density of points (see section 4 below), we find values for z that are very small for all the β we have measured. We have not, of course, pinpointed the transition point accurately with the current batch of simulations so it would be unwise to claim that critical slowing down is almost eliminated on dynamical lattices with the

[#1] We restrict ourselves to the rough phase as the correlation length ξ is effectively the linear lattice size here – in the smooth phase we would have to fit to the exponential decay of a two-point function to obtain ξ.

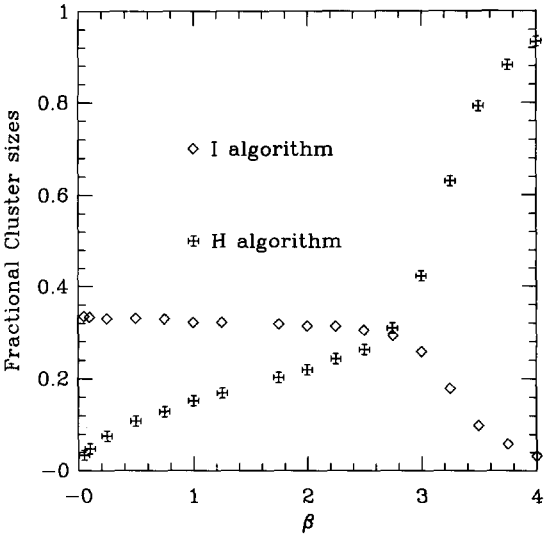

Fig. 3. The mean cluster sizes as a fraction of the lattice size for the two cluster algorithms on the largest (N = 10000) graphs simulated.

cluster algorithms used here – we would need data at the critical point to assure us of this. Nonetheless, it would appear that a small value of z is likely to be achieved there too, judging from the persistently low values for all the measured β.

The behaviour of the cluster algorithms as β is varied is shown in fig. 3, where the average cluster size as a fraction of the total number of lattice points is plotted. In the critical region ($\beta \simeq 3$) both the H and I algorithms generate clusters of approximately the same *average* fractional size. This is slightly misleading as a closer look at the cluster statistics reveals that the I algorithm produces more clusters of intermediate size than the H algorithm, which tends to favour both very large and very small clusters. This behaviour is similar to that of the clusters on a fixed lattice.

There is an interesting crossover in the average cluster sizes of the two algorithms in the region of the phase transition point. Deep in the rough phase at low β the H algorithm produces a small average cluster size with fewer clusters generated per attempt. This is because at low β there is a good chance that the random reflection plane picked will be a long way from the seed point in the H algorithm, so the cluster growing will fail at the first step because of the large penalty in the probability factor. The I algorithm, on the other

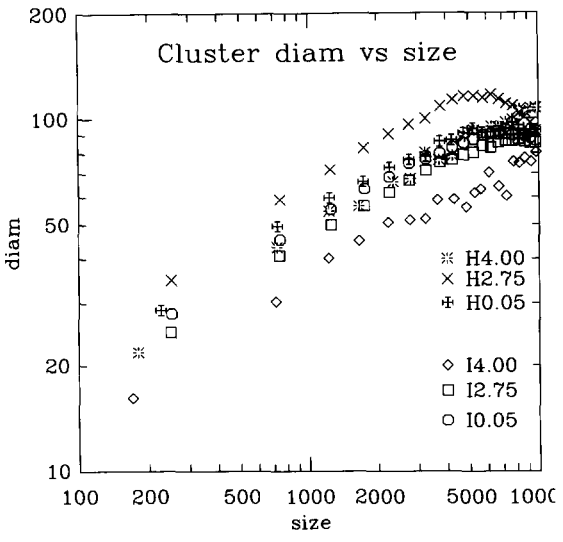

Fig. 4. Binned sizes of both H and I clusters on $N = 10000$ lattices plotted against their diameters on a log/log scale for selected β.

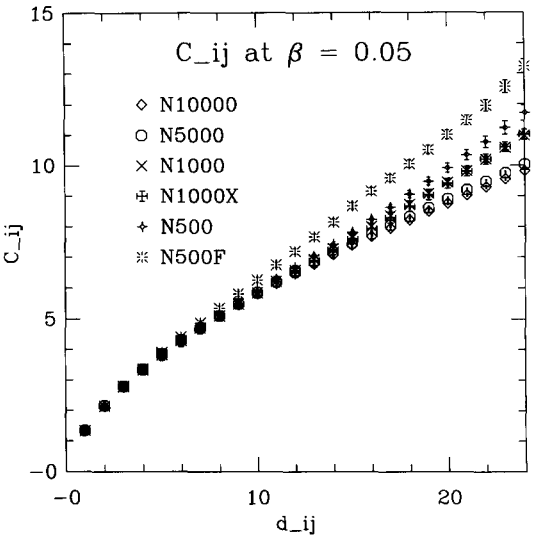

Fig. 5. The correlator C_{ij} at $\beta = 0.05$ for various lattice sizes. Additional simulations of a *real* gaussian scalar field X on a dynamical lattice with 1000 points and an h field on a *fixed* lattice with 500 points are shown as $N1000X$ and $N500F$ respectively.

hand, always picks a point at distance 1/2 from the seed and incurs no such penalty. In the smooth phase ($\beta \geqslant 3$) the situation is reversed – we now see that the H algorithm generates clusters almost the size of the graph, whereas the I algorithm has a small average size. The histogram of the cluster sizes reveals that the H algorithm produces clusters almost the size of the graph at most attempts, whereas the I algorithm has a very much smaller peak for clusters of this size and fails to build a cluster with much greater probability. This is presumably because the I algorithm is more likely to encounter a point on the opposite side of the reflection plane for a thin surface at an early stage and terminate the cluster growth.

We have also measured the size and diameter of the clusters grown and binned values for these on an $N = 10000$ lattice, without error bars for clarity, are plotted against each other on log–log scales for three β values in fig. 4. The H and I clusters behave differently with temperature – the curves for the I clusters shift monotonely upwards with temperature, but the highest curve for the H clusters is roughly in the critical region at $\beta = 2.75$. In spite of this variation the slopes in the linear section of the graphs are almost constant, which gives a fractal dimension (with a large error due to the spread in the individual clusters) of 2.5 similar to that measured naively for the graphs themselves as discussed in section 4 below.

The results of the measurements on the correlator C_{ij} are plotted in fig. 5 for $\beta = 0.05$. As we are deep in the rough phase we would expect essentially free-field behaviour, which naively suggests a logarithmic growth with $d_{ij} = |i - j|$. However, we see that the growth is actually *linear* after an initial logarithmic section which increases with the lattice size. The form of the curve is similar on fixed lattices where the flips are switched off, even though the slope changes slightly, so we are clearly looking at a finite size effect caused by the spherical topology. Further evidence for this interpretation is provided by simulating a single free scalar field with a gaussian action, which gives identical behaviour to the h, as it should for small β. Although the complicated fractal nature of the ϕ^3 graphs makes naive geometrical arguments rather dangerous, it is possible to construct a plausibility argument for such behaviour: the scalar propagator (i.e. effectively our correlator) on a sphere can be written as $\log|z|$ where $|z|$ is the stereographically projected distance from the sphere on the complex plane. This is related to the distance d_{ij} we measure on the sphere by

$$\frac{|z|}{2R} = \frac{(d_{ij}/\pi R)}{\sqrt{1-(d_{ij}/\pi R)^2}}, \tag{17}$$

where R is the radius of the sphere. If $\log|z(d_{ij})|$ is plotted as a function of d_{ij}, which is what we are doing when we measure the correlator, it has a long quasi-linear portion after the initial logarithmic increase.

4. Lattice properties

The results of the measurements of the lattice properties are succinctly summarized in fig. 6, which should be compared with the similar fig. 5 in our earlier simulations of the XY model [11]. The measured quantities AL and AF relate to the acceptance of the flip moves on the graphs. A flip can be forbidden either from constraints arising from the graph (i.e. no tadpoles and no self-energy bubbles) or from the energy change in the spin model induced by the reconnection of the vertices. AL measures the fraction of randomly selected links which pass the first test and could be flipped according to the graph constraints and AF measures the fraction of the links satisfying the graph constraints that actually are flipped, i.e. pass the Metropolis test using the DGSOS model energy change. Also plotted is the fraction of rings of length 3, PR3, which serves as an indicator of the local curvature distribution in the ϕ^3 graph.

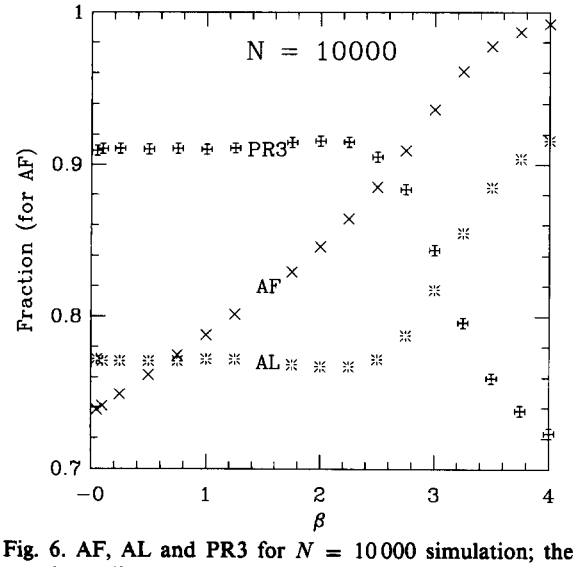

Fig. 6. AF, AL and PR3 for $N = 10000$ simulation; the y-scale applies to AF only, AL and PR3 have been scaled appropriately to fit on plot.

From fig. 6 it is clear that PR3 has a modest peak in the region of the phase transition, with a dip appearing in AL at the same point. This behaviour appears to be generic in all the models on dynamical lattices that we have simulated. However, there is no sign of the universality with the central charge, c, of the various lattice properties that we found in the Potts model simulations [6] where the curves of AL, AF and PR3 as functions of the reduced temperature depended only on c and the maximum and phase transition values of PR3 grew linearly with c. This is not surprising as the XY model also failed to show these properties. It is interesting to note, however, that the DGSOS model displays clearly different lattice properties to even the XY model. In particular AF is monotone increasing for the DGSOS model whereas it is rather similar in form to AL in the XY model with a dip occurring well below the phase transition point. In view of the duality between the XY and an (admittedly slightly different) SOS model one might have expected simply reversing left and right in fig. 6 to have reproduced the XY model results. In addition the maximum value of PR3 observed for the DGSOS model is 0.2211 at $\beta = 2.00$, which should be compared with 0.2185 for the XY model on graphs of a similar size.

We have also attempted a naive measurement of the fractal dimension of the lattice by simply counting the number of points $N(r)$ within a given geodesic distance r of a random starting point i,

$$N(r) = \left\langle \sum_{ij} \theta(r - d_{ij}) \right\rangle, \tag{18}$$

and using $\log N(r) \simeq d \log r$ to extract the fractal dimension d. A similar procedure gave values in the region of 2.7 for Potts models when extrapolated to infinite lattice size and 2.6 for the XY model when extrapolated in a self-consistent fashion [6,11]. Applying the same methods to the DGSOS model lattices again produces a value in the region of 2.6. However, the recent work of Kawai et al. on a transfer matrix formalism for pure 2d gravity [15] shows that a direct measurement of the density of points such as we have carried out here contains non-universal, lat-

tice dependent factors [#2]. This is likely to remain true with the introduction of matter so, while our results may be useful for comparing the behaviour of different models on similar lattices, it is unclear how reliable they are as measurements of the "dimension" of the lattices.

5. Conclusions

We have simulated a DGSOS model on dynamical ϕ^3 graphs using a mixed cluster algorithm. There is good evidence for the logarithmic growth of the width-squared of the surface in the rough phase predicted by KT theory. The energy and specific heat of the DGSOS model also have the expected forms and low β limits. Measurements of the dynamical critical exponent suggest that critical slowing down may well be eliminated completely, though it would take an accurate determination of the critical point to be absolutely certain of this. The lattice properties we observed are *not* a simple inversion of those seen in the XY model, which is dual to a slightly different sort of SOS model. It would be interesting to obtain more data in the critical region with the DGSOS model and fit to the improved formula for the width-squared in order to determine the critical β accurately. It would also be interesting to look at the dual to the XY model to see if the lattice properties there are then closer to a straightforward reflection of those in the XY model. As SOS surfaces are in effect Gauss parametrizations of 2d surfaces embedded in 3d with no overhangs it would be very useful if cluster algorithms similar to those used here could be devised for the more complicated actions including extrinsic curvature that are used in simulations of "real" surfaces and string theory.

Acknowledgement

This work was supported in part by NATO collaborative research grant CRG910091 (C.F.B. and D.A.J.) and by ARC grant 313-ARC-VI-92/37/scu (W.J. and D.A.J.). C.F.B. is supported by DOE under contract DE-FG02-91ER40672 and by NSF Grand Challenge Applications Group Grant ASC-9217394, and W.J. thanks the Deutsche Forschungsgemeinschaft for a Heisenberg fellowship. DAJ is supported at LPTHE by an EEC HCM fellowship. The simulations were carried out on workstations at Heriot-Watt University and Mainz.

[#2] This accounts for the earlier results of [16], which failed to find *any* fractal dimension on very large bare lattices.

References

[1] V.G. Knizhnik, A.M. Polyakov and A.B. Zamolodchikov, Mod. Phys. Lett. A 3 (1988) 819.

[2] F. David, Mod. Phys. Lett. A 3 (1988) 1651;
J. Distler and H. Kawai, Nucl. Phys. B 321 (1989) 509.

[3] For a review see P. Ginsparg, Matrix Models of 2d Gravity, Trieste Lectures 1991, LA-UR-91-9999, hep-th 9112013.

[4] V.A. Kazakov, Phys. Lett. A 119 (1986) 140;
D.V. Boulatov and V.A. Kazakov, Phys. Lett. B 186 (1987) 379.

[5] J. Jurkiewicz, A. Krzywicki, B. Petersson and B. Soderberg, Phys. Lett. B 213 (1988) 511;
R. Ben-Av, J. Kinar and S. Solomon, Nucl. Phys. B (Proc. Suppl.) 20 (1991) 711;
S.M. Catterall, J.B. Kogut and R.L. Renken, Phys. Rev. D 45 (1992) 2957;
C.F. Baillie and D.A. Johnston, Mod. Phys. Lett. A 7 (1992) 1519.

[6] C.F. Baillie and D.A. Johnston, Phys. Lett. B 286 (1992) 44.

[7] J. Ambjørn, B. Durhuus and T. Jonsson, Matter Fields with $c > 1$ Coupled to 2-d Gravity, NBI-HE-92-35, hep-th 9208030;
S.M. Catterall, J.B. Kogut and R.L. Renken, Phys. Lett. B 292 (1992) 277;
S. Hikami, Phys. Lett. B 305 (1993) 327;
E. Brézin and S. Hikami, Phys. Lett. B 295 (1992) 209; B 283 (1992) 203.

[8] J.M. Kosterlitz and D.J. Thouless, J. Phys. C 6 (1973) 1181;
J.M. Kosterlitz, J. Phys. C 7 (1974) 1046;
V.L. Berezinski, JETP 34 (1972) 610.

[9] R. Gupta, J. DeLapp, C.G. Batrouni, G.C. Fox, C.F. Baillie and J. Apostolakis, Phys. Rev. Lett. 61 (1988) 1996;
U. Wolff, Nucl. Phys. B 322 (1989) 759;
R.G. Edwards, J. Goodman and A.D. Sokal, Nucl. Phys. B 354 (1991) 289;
R. Gupta and C.F. Baillie, Phys. Rev. B 45 (1992) 2883;
H. Evertz, M. Hasenbusch, M. Marcu, K. Pinn and S. Solomon, J. Phys. I (France) 1 (1991) 1669;
W. Janke and K. Nather, Phys. Lett. A 157 (1991) 11; Phys. Rev. B 48 (in press).

[10] D. Gross and I. Klebanov, Nucl. Phys. B 344 (1990) 475; B 354 (1991) 459;
D.V. Boulatov and V.A. Kazakov, Nucl. Phys. B (Proc. Suppl.) 25A (1992) 38.
[11] C.F. Baillie and D.A. Johnston, Phys. Lett. B 291 (1992) 233.
[12] S.M. Catterall, J.B. Kogut and R.L. Renken, The XY Model on a Dynamical Random Lattice, ILL-(TH)-93-5, DAMTP-93-16, hep-lat 9304015.
[13] R. Baxter, Exactly solved Models in Statistical Mechanics (Academic Press, 1982).
[14] H. Evertz, M. Hasenbusch, M. Marcu, K. Pinn and S. Solomon, Int. J. Mod. Phys. C 3 (1992) 235; Phys. Lett. B 254 (1991) 185;
H. Evertz, M. Hasenbusch, M. Marcu and K. Pinn, Nucl. Phys. B (Proc. Suppl.) 20 (1991);
The Solid on Solid Surface Width Around The Roughening Transition, CERN-TH.6893/93, cond-mat 9305029.
[15] H. Kawai, N. Kawamoto, T. Mogami and Y. Watakibi, Phys. Lett. B 306 (1993) 19.
[16] M. Agishtein and A. Migdal, Nucl Phys. B 350 (1991) 690.